

Electronic Supplementary Information

Co₃O₄@PEI/Ti₃C₂T_x MXene nanocomposites for highly sensitive NO_x gas sensor with low detection limit

Baihe Sun ^{#a}, He Lv^{#a}, Zhusuo Liu^a, Jue Wang^a, Xue Bai^a, Yang Zhang^a, Junkun Chen^a, Kan Kan^{*b}, and Keying Shi^{*a}

^a Key Laboratory of Functional Inorganic Material Chemistry, Ministry of Education. School of Chemistry and Material Science, Heilongjiang University, Harbin, 150080, P. R. China. E-mail: shikeying2008@163.com

^b Heilongjiang Academy of Sciences, Institute of Advanced Technology, Harbin 150020, P. R. China. E-mail: kankan.has@foxmail.com

[#] These authors contributed equally to this work.

Table S1 Comparison of the gas sensing characteristics of MXene based materials reported in literature and in present work.

Sensor material	Operating temperature	Gas	Response/ Gas concentration	Response time	Recovery time	Detection limit	Ref.
Delaminated $\text{Ti}_3\text{C}_2\text{T}_x$ MXene	RT	H_2O	26.1/ 80±5%	-	-	-	21
Metallic $\text{Ti}_3\text{C}_2\text{T}_x$ MXene	RT	ethanol	1.7/ 100 ppm	-	-	100 ppb	22
TiO_2 / $\text{Ti}_3\text{C}_2\text{T}_x$	RT	NH_3	3.1%/ 10 ppm	33 s	277 s	-	23
PANI/ $\text{Ti}_3\text{C}_2\text{T}_x$	RT	ethanol	41.1%/ 200 ppm	0.4 s	0.5 s	-	24
MXene@Pd CNC film	RT	H_2	23±4%/4%	32±7 s	-	-	25
$\text{W}_{18}\text{O}_{49}/\text{Ti}_3\text{C}_2\text{T}_x$	300 °C	acetone	11.6/ 20 ppm	5.6 s (170 ppb)	6 s (170 ppb)	170 ppb	26
$\text{TiO}_2/\text{Ti}_3\text{C}_2$ Mxene	RT	NO_2	16.02%/ 5 ppm	-	-	125 ppb	28
3D $\text{Ti}_3\text{C}_2\text{T}_x/\text{ZnO}$ spheres	RT	NO_2	41.93%/ 100 ppm	34 s	103 s	-	29
Alkalized $\text{Ti}_3\text{C}_2\text{T}_x$	RT	NH_3	28.87%/ 100 ppm	-	-	-	35
3D Mxene framework	RT	ethanol	4.4%/ 5 ppm	Less than 12 s	Less than 12s	50 ppb	44
$\text{CuO}/\text{Ti}_3\text{C}_2\text{T}_x$	250 °C	toluene	11.4/ 50 ppm	270 s	10 s	-	S1
MXene/SnO ₂	RT	NH_3	40%/ 50 ppm	36 s	44 s	-	S2
PSS/MXene composites	RT	NH_3	36.6%/ 100 ppm	116 s	40 s	-	S3
single-layer Ti_3C_2 - MXene	RT	NH_3	6.13%/ 500 ppm	-	-	10 ppm	S4
30ppb (experiment) 12.7ppb (theory)							This work
CoPM-24	RT	NO_x	27.9/100 ppm	2 s	73 s		

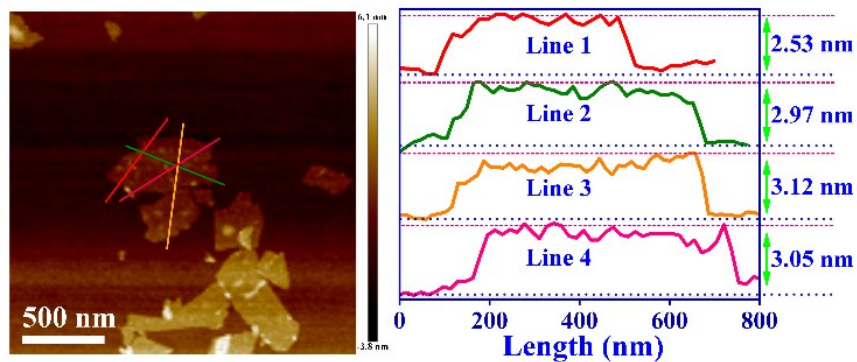


Fig. S1 AFM images and height profiles of $\text{Ti}_3\text{C}_2\text{T}_x$ MXene nanosheets.

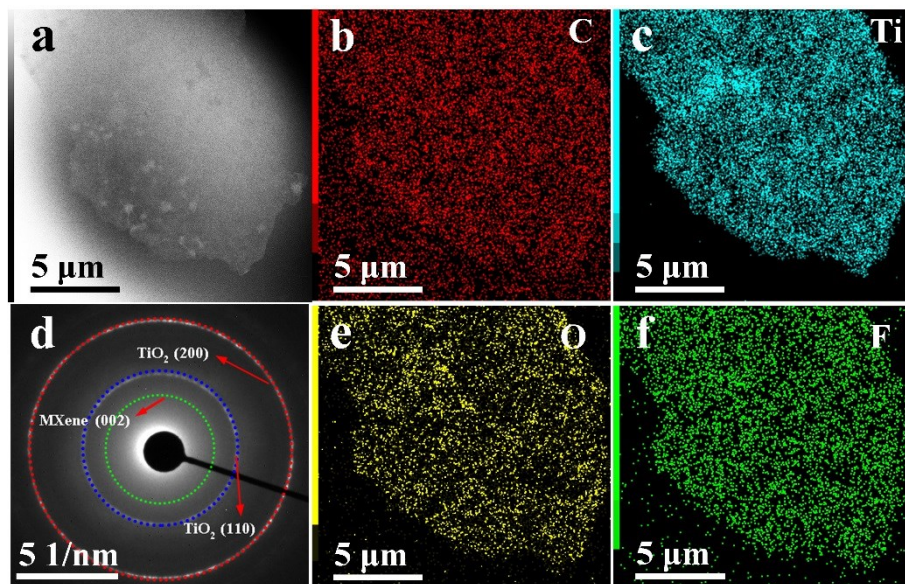


Fig. S2 TEM images (a) and EDS elemental mapping analysis (b-c, e-f) and EDS image (d) of $\text{Ti}_3\text{C}_2\text{T}_x$ MXene.

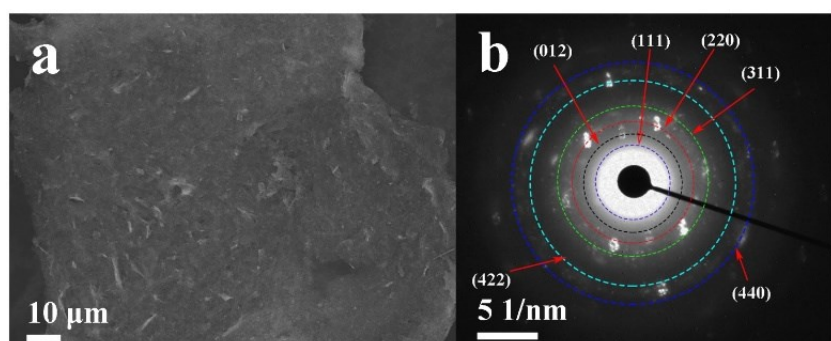


Fig. S3 SEM images (a) and SAED (b) of CoPM-24.

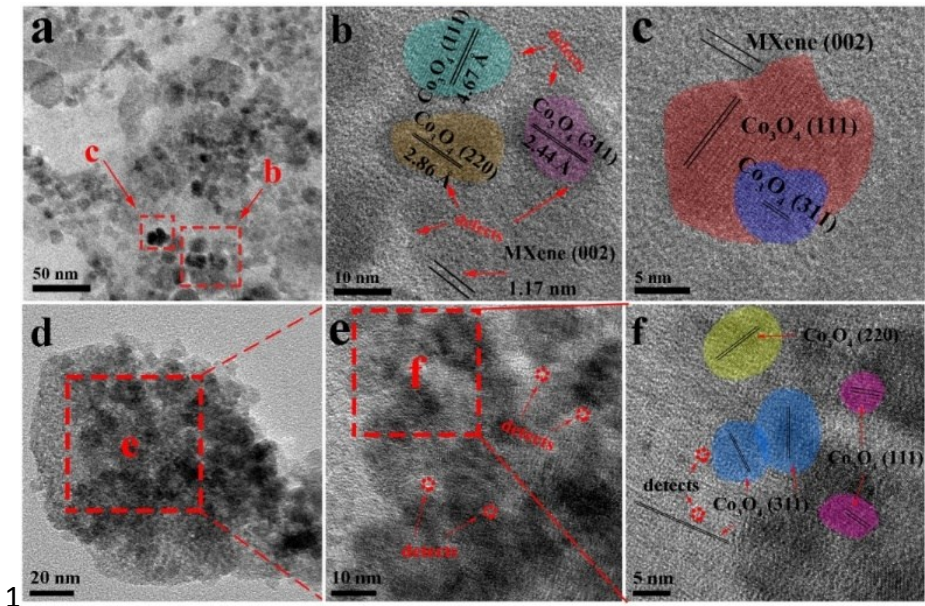


Fig. S4 TEM and HRTEM images of the CoPM-18 (a-c) and CoPM-30 (d-f).

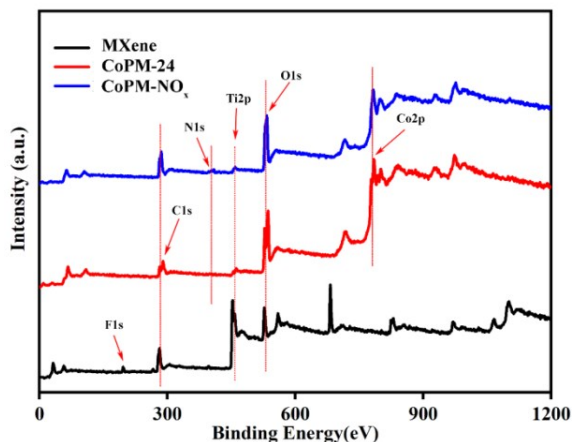


Fig. S5 XPS survey spectra of $\text{Ti}_3\text{C}_2\text{T}_x$ MXene, CoPM-24 and CoPM- NO_x .

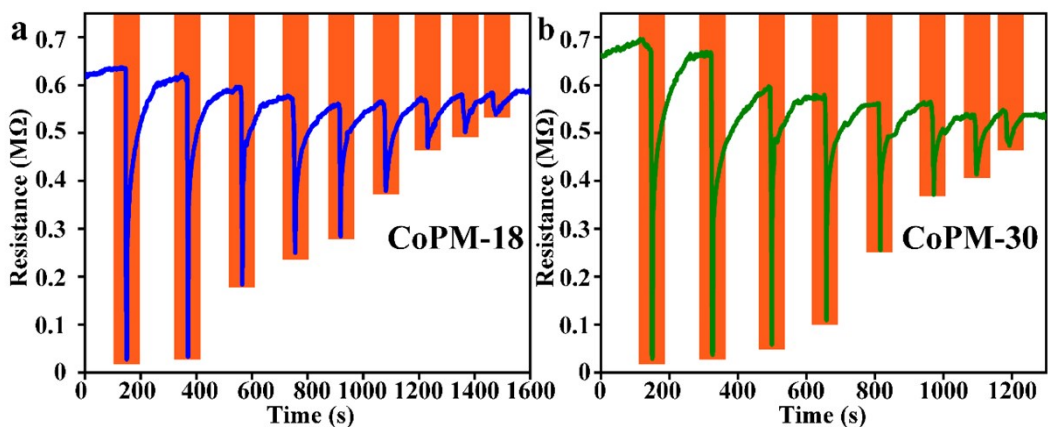


Fig. S6 Dynamic response-recovery curve of (a) CoPM-18 and (b) CoPM-30 sensors.

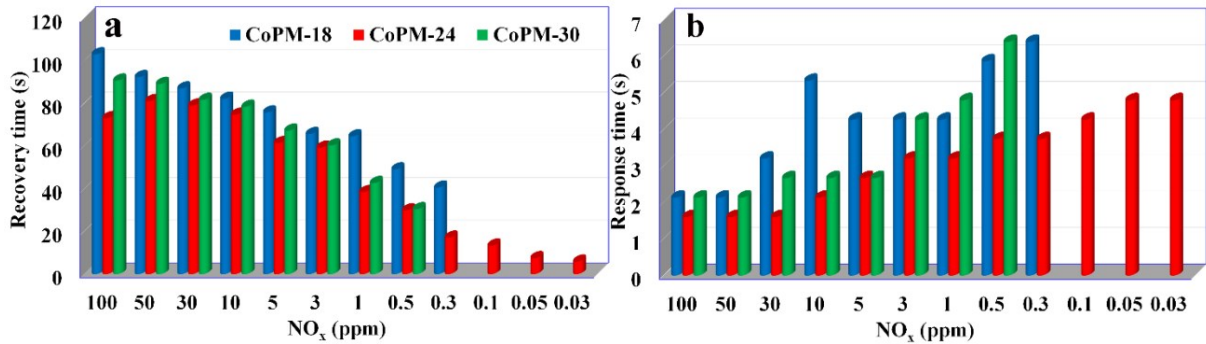


Fig. S7 the response times (a) and the recovery times (b) of CoPM-18, CoPM-24 and CoPM-30 sensors.

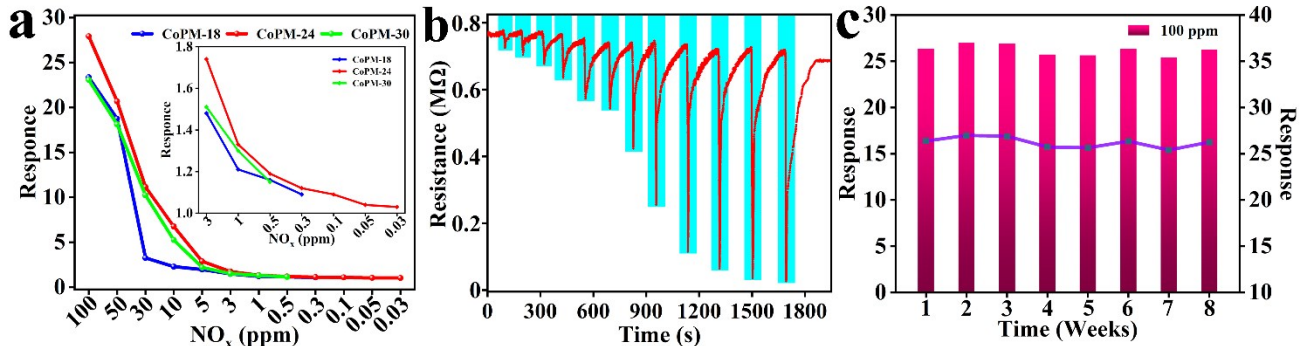


Fig. S8 The gas sensitive line chart (a), the transient dynamical responses to 0.03 ~ 100 ppm NO_x (b), the stability to 100 ppm NO_x gases detecting day for 8 weeks (c) of the CoPM-24 sensor.

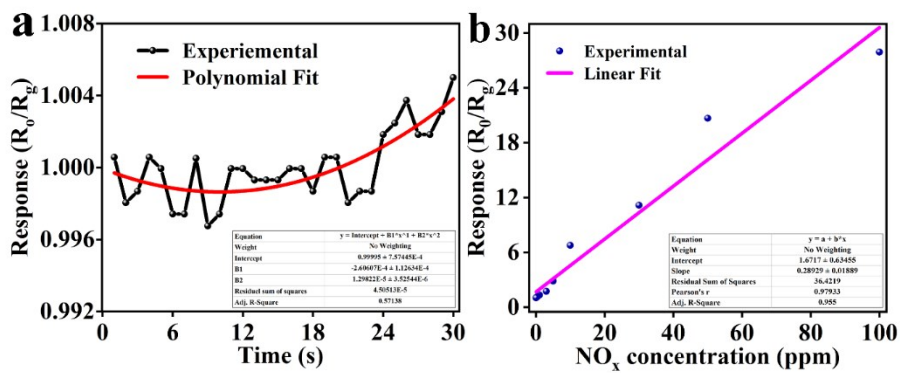


Fig. S9 (a) The curve with detailed data obtained by polynomial fitting the first 30 response points in the response-time baseline of the CoPM-24 gas sensor before the injection of NO_x . The response values before and after fitting are recorded as Si and S, respectively, (b) the curve with detailed data obtained by linear fitting the response points in the NO_x sensing measurement of Fig. 5d.

Calculation for limit of detection (LOD):

The theoretical LOD were calculated using the variation in the gas response at base line using the root mean square deviation (rms noise). For polynomial fitting, we took 30 experimental data point from Fig. 5a. According to the formula (1) below, and S_i and S obtained by the polynomial fit method in Fig. S9a, Vx^2 can be calculated as follow.

[S5, S6]

$$Vx^2 = \Sigma(S_i - S)^2 \quad (1) [S5, S6]$$

$$Vx^2 = 0.00004496$$

In terms of the root mean square (rms), i.e., formula (2), rms_{noise} can be calculated as follows.

$$rms = \sqrt{Vx^2/n} \quad (n = 20) \quad (2) [S5, S6]$$

$$rms = 0.00122$$

Finally, according to the formula (3) and the value of slope (0.28929) obtained from Fig. S9b, the theoretic Limit of detection (LOD) can be calculated:

$$LOD = 3 * (rms/slope) \quad (3) [S5, S6]$$

$$LOD = 0.0127 \text{ ppm or } 12.7 \text{ ppb}$$

Therefore, the theoretical detection limit of 12.7 ppb to NO_x at RT.

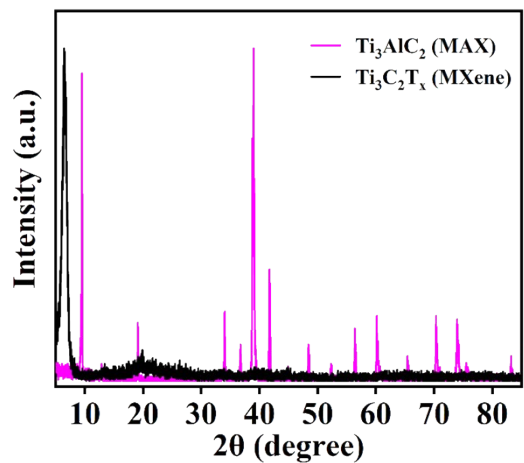


Fig. S10 XRD patterns of Ti_3AlC_2 (MAX) and $\text{Ti}_3\text{C}_2\text{T}_x$ (MXene).

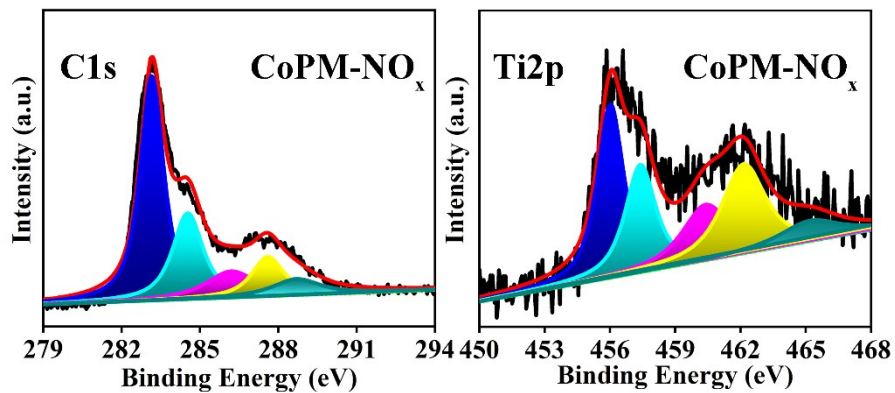


Fig. S11 XPS spectra of CoPM-24 in NO_x adsorption (a) C1s XPS spectra; (b) Ti2p XPS spectra

Table S2 Response, response time and recovery time of CoPM-18, CoPM-24 and CoPM-30 sensors.

Sensors	CoPM-18			CoPM-24			CoPM-30		
NO ₂ (ppm)	R	T _s	T _r	R	T _s	T _r	R	T _s	T _r
100	23.35	2.13	102.93	27.92	1.60	73.07	23.06	2.13	90.67
50	18.75	2.13	92.27	20.68	1.60	81.07	18.12	2.13	89.07
30	3.25	3.20	86.93	11.15	1.60	78.93	10.23	2.67	81.60
10	2.29	5.33	82.13	6.76	2.13	74.67	5.26	2.67	78.40
5	1.97	4.27	75.73	2.87	2.67	61.33	2.20	2.67	67.20
3	1.48	4.27	65.60	1.74	3.20	59.20	1.51	4.27	60.27
1	1.21	4.27	64.53	1.33	3.20	38.40	1.30	4.80	42.67
0.5	1.16	5.87	49.07	1.19	3.73	29.87	1.15	6.40	30.40
0.3	1.09	6.40	40.53	1.12	3.73	17.07			
0.1				1.09	4.27	13.33			
0.05				1.04	4.80	7.47			
0.03				1.03	4.80	5.87			

*R: Response T_s: Response time T_r: Recovery time

Table S3 Peaks positions (eV) of the XPS analysis results to Pure MXene, CoPM-24 and CoPM-NO_x

Elements	Peak position (eV)		
	MXene	CoPM-24	CoPM-NO _x
Ti2p	455.2, 456.6, 459.3, 461.6 and 464.7	455.6, 456.9, 460.1, 461.8 and 464.8	456.0, 457.4, 460.4, 462.2 and 465.2
	282.0, 283.5, 286.5 and 288.0	282.4, 283.7, 285.8, 286.9 and 288.8	283.2, 284.6, 286.3 287.6 and 288.9
O1s	530.3, 531.7 and 532.9	530.4, 532.0 and 534.9	532.0, 533.3 and 535.6
Co2p	-	779.1, 781.8, 785.6, 795.3, 800.1 and 803.4	779.8, 782.9, 786.6, 795.8, 800.3 and 804.2
	-	398.5	399.4, 404.0 and 407.6

References

- S1. A. Hermawan, B. Zhang, A. Taufik, Y. ASakura, T. Hasegawa, J. Zhu, P. Shi and S. Yin, *ACS Appl. Nano Mater.*, 2020, 3, 4755–4766.
- S2. T. He, W. Liu, T. Lv, M. Ma, Z. Liu, A Vasiliev and X. Li, *Sens. Actuators, B*, 329 (2021) 129275.
- S3. L. Jin, C. Wu, K. Wei, L. He, H. Gao, H. Zhang, K Zhang, A. M. Asiri, K. A. Alamry, L. Yang and X. Chu, *ACS Appl. Nano Mater.*, 2020, 3, 12071–12079.
- S4. M. Wu, M. He, Q. Hu, Q. Wu, G. Sun, L. Xie, Z. Zhang, Z. Zhu and A. Zhou, *ACS Sens.*, 2019, 4, 2763–2770.
- S5. V. Dua, S. P. Surwade, S. Ammu, S. R. Agnihotra, S. Jain, K. E. Roberts, S. Park, R. S. Ruoff, and S. K. Manohar, *Angew. Chem.*, 2010, 122, 2200 –2203.
- S6. J. Li, Y. Lu, Q. Ye, M. Cinke, J. Han and M. Meyyappan, *Nano Lett.*, Vol. 3, No. 7, 2003.